

PAPER • OPEN ACCESS

## Nanoengineered Surfaces for Thermal Energy Conversion

To cite this article: Bikram Bhatia *et al* 2015 *J. Phys.: Conf. Ser.* **660** 012036

View the [article online](#) for updates and enhancements.

You may also like

- [A Review on Thermophotovoltaic Energy Conversions and its Space Power Applications](#)  
Jagannath Nayak and Deepak Kumar
- [Investigation into the structure–property relationship and technical properties of TPEs and TPVs derived from ethylene octene copolymer \(EOC\) and polydimethyl siloxane \(PDMS\) rubber blends](#)  
R Padmanabhan, Kinsuk Naskar and Golok B Nando
- [Unidirectional radiative heat transfer with a spectrally selective planar absorber/emitter for high-efficiency solar thermophotovoltaic systems](#)  
Asaka Kohiyama, Makoto Shimizu and Hiroo Yugami



**ECS**  
The  
Electrochemical  
Society  
Advancing solid state &  
electrochemical science & technology

**DISCOVER**  
how sustainability  
intersects with  
electrochemistry & solid  
state science research

# Nanoengineered Surfaces for Thermal Energy Conversion

**Bikram Bhatia, Daniel J. Preston, David M. Bierman, Nenad Miljkovic, Andrej Lenert, Ryan Enright, Youngsuk Nam, Ken Lopez, Nicholas Dou, Jean Sack, Walker R. Chan, Ivan Celanović, Marin Soljačić and Evelyn N. Wang**

Massachusetts Institute of Technology, Cambridge, MA, USA

E-mail: enwang@mit.edu

**Abstract.** We provide an overview of the impact of using nanostructured surfaces to improve the performance of solar thermophotovoltaic (STPV) energy conversion and condensation systems. We demonstrated STPV system efficiencies of up to 3.2%, compared to  $\leq 1\%$  reported in the literature, made possible by nanophotonic engineering of the absorber and emitter. For condensation systems, we showed enhanced performance by using scalable superhydrophobic nanostructures *via* jumping-droplet condensation. Furthermore, we observed that these jumping droplets carry a residual charge which causes the droplets to repel each other mid-flight. Based on this finding of droplet residual charge, we demonstrated electric-field-enhanced condensation and jumping-droplet electrostatic energy harvesting.

## 1. Introduction

All thermal energy conversion processes are governed by the three modes of heat transfer: conduction, convection and radiation. Nanoengineered surfaces can influence each of these three modes resulting in efficiency enhancements in a variety of energy conversion systems. This work focuses on the application of nanoengineered surfaces in two areas: solar thermophotovoltaic (STPV) energy conversion and condensation heat transfer.

Existing approaches used to generate power from sunlight use either photovoltaics, in which sunlight directly excites electron-hole pairs in a semiconductor, or solar-thermal, in which sunlight drives a mechanical heat engine. Photovoltaic power generation is intermittent and typically only exploits a portion of the solar spectrum efficiently, whereas the intrinsic irreversibilities of small heat engines make the solar-thermal approach best suited for utility-scale power plants. There is, therefore, an increasing need for hybrid technologies, such as STPV, that can combine photovoltaics and solar-thermal to harness the entire solar-spectrum.

Unlike STPV which is a nascent solar energy conversion approach, condensation is a ubiquitous process often observed in nature and harnessed in many industrial processes such as power generation, desalination, thermal management, and building environmental control. Recent advances in surface engineering have offered new opportunities to enhance condensation heat transfer by drastically changing the wetting properties of the condenser surface. Specifically, the development of superhydrophobic surfaces has been pursued to enhance condensation heat transfer, where the low droplet surface adhesion and small droplet departure sizes increase the condensation heat transfer coefficient. Additionally, more detailed insights on droplet interactions on these surfaces can lead to new opportunities for a wide variety of possible applications including self-cleaning, anti-icing, and energy harvesting [1].



## 2. Solar thermophotovoltaic energy conversion

A solar thermophotovoltaic device converts sunlight into thermal emission tuned to energies directly above the photovoltaic bandgap using a hot absorber–emitter. By doing so, solar thermophotovoltaics promise to achieve high efficiency, by harnessing the entire solar spectrum; scalability and compactness, because of their solid-state nature; and dispatchability, owing to the ability to store energy using thermal or chemical means. However, efficient collection of sunlight in the absorber and spectral control in the emitter are particularly challenging at high operating temperatures which has limited previous experimental demonstrations of this approach to conversion efficiencies around or below 1% [2]. STPV systems with structured surfaces with tailored spectral properties were theoretically predicted to achieve efficiencies exceeding 40%, however no such experimental demonstration has been reported in the literature. We developed a full solar thermophotovoltaic device consisting nanoengineered absorber and emitter surfaces that enabled us to reach experimental efficiencies of 3.2% [3].

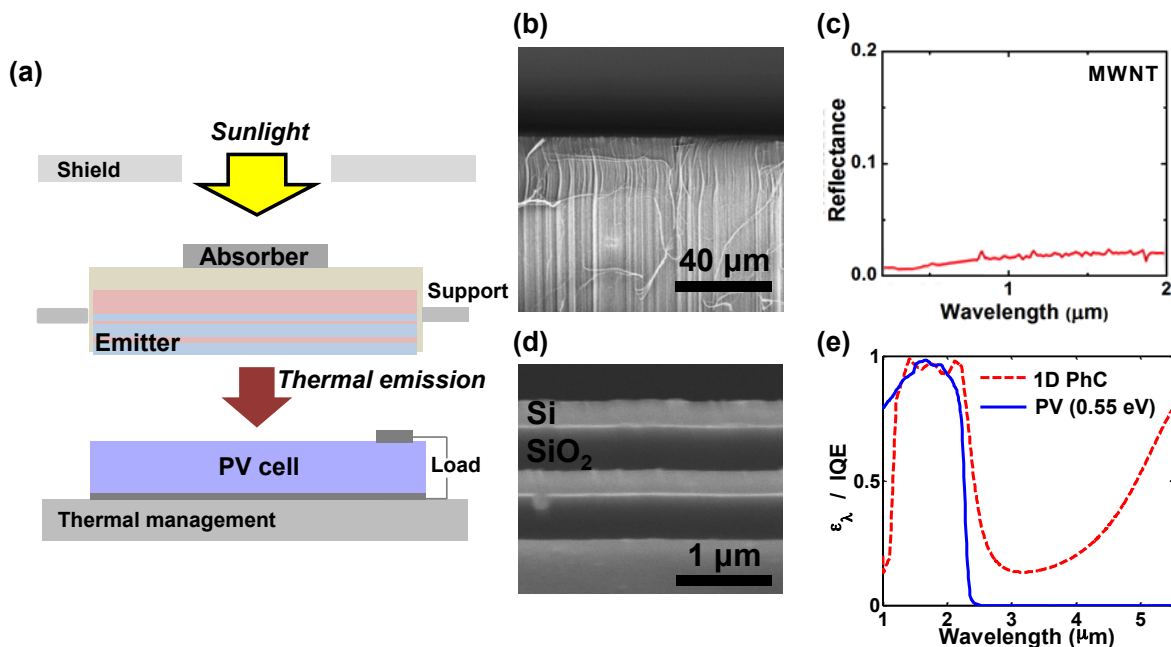


**Figure 1.** (a) Schematic of our vacuum-enclosed devices composed of an aperture/radiation-shield, an array of MWNTs as the absorber, a 1D PhC, a 0.55 eV-bandgap photovoltaic cell (InGaAsSb) and a chilled water cooling system. (b) SEM cross-section of the MWNTs. (c) Measured optical reflectance of the MWNT absorber. (d) SEM cross-section of the 1D PhC showing the alternating layers of silicon and SiO<sub>2</sub>. (e) Measured emittance of the PhC emitter (red) and internal quantum efficiency of the InGaAsSb PV cell (blue) plotted as a function of wavelength. (Adapted from [3])

Figure 1a shows a schematic of our STPV device that integrates a multiwalled carbon nanotube (MWNT) absorber and a one-dimensional Si/SiO<sub>2</sub> photonic-crystal (PhC) emitter. Thermal resistance between the absorber and emitter is minimized by integrating the absorber and emitter on the same conductive silicon substrate such that heat is effectively delivered to the emitter via thermal spreading. In addition, we varied the absorber–emitter areas to tune the energy balance of the device. The absorber area is reduced with respect to the planar area of the sample, so we supply enough heat for the absorber–emitter to reach optimal emitter temperature by increasing the level of irradiance and leveraging the high absorptance of the nanotube array. Emitter-to-absorber area ratios (AR) >1 also reduced the area for remissive losses from the nearly blackbody nanotube array surface, thus boosting

thermal efficiency. To reduce parasitic radiative losses, we metallized the sides of the silicon substrate and inactive area around the nanotube absorber with tungsten, a relatively low-emissivity, high-temperature material, and incorporated a high-reflectivity silver-coated shield (Figure 1a) to recycle this parasitic radiation back to the device.

Vertically aligned carbon nanotubes were chosen as the solar absorber because of their high-temperature stability in vacuum and their nearly ideal absorptance, crucial for absorbing highly concentrated irradiance at elevated emitter-to-absorber area ratios. As shown in Figure 1b, the as-grown nanotubes are 10–15 nm in outer diameter and 80–100  $\mu\text{m}$  tall, with a  $\pm 0.5 \mu\text{m}$  variation in height at the tips. The broad-spectrum absorptance of the nanotube array in this study exceeds 0.99 (Figure 1c), consistent with previous reports for similar nanotube array geometries.

The multilayer Si/SiO<sub>2</sub> structure of the 1D photonic crystal, composed of five alternating layers of silicon and SiO<sub>2</sub> (Figures 1d,e), improves the spectral matching between the emittance of the emitter and the internal quantum efficiency of the InGaAsSb photovoltaic cell ( $E_g = 0.55 \text{ eV}$ ). These materials were chosen for ease of fabrication and high-temperature compatibility with the silicon substrate. The layer thicknesses were optimized via a constrained global optimization of the product of efficiency and power density.

Figure 2 shows the thermal-to-electrical conversion efficiency ( $\eta_t \eta_{\text{tpv}}$ ) plotted as a function of input solar irradiance  $H_s$ . Overall, the highest conversion efficiency we measured was  $3.2 \pm 0.2\%$  using an AR = 7 device, which is three times greater than that obtained in previous STPV experiments. This was achieved using a compact design at substantially lower levels of optical concentration ( $\sim 750$  times), which enables higher optical efficiencies. Significant enhancements in efficiency relative to a greybody absorber–emitter ( $\epsilon = 0.5$ ) were achieved through the use of (1) a 1D PhC for improved spectral performance of the emitter and a vertically aligned MWNT array for nearly ideal solar absorptance (a twofold contribution to the improvement in  $\eta_t \eta_{\text{tpv}}$ ) and (2) optimization of the active emitter-to-absorber area ratio (an additional twofold improvement).

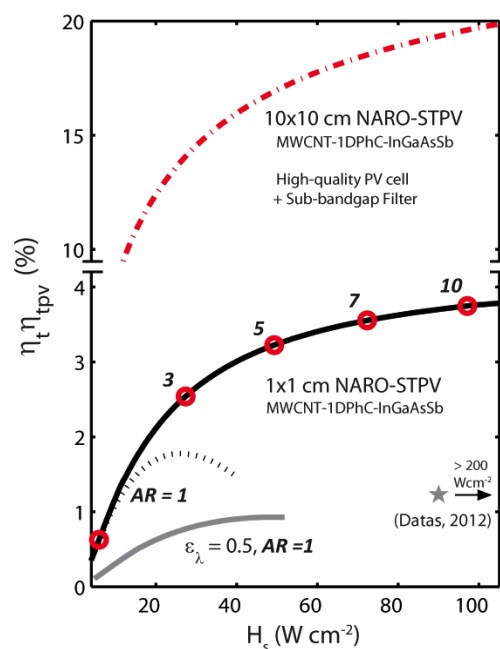


**Figure 2.** Relative improvements in efficiency and near-term predictions for nanophotonic STPVs. Conversion efficiency  $\eta_{\text{th}} \eta_{\text{pv}}$  as a function of a solar irradiance  $H_s$ . Red symbols show experimental results with devices different AR (values specified next to symbols) and solid lines represent modeling results. Efficiencies approaching 20% were predicted with a scaled-up ( $10 \times 10 \text{ cm}^2$ ) STPV device utilizing a high-quality 0.55 eV photovoltaic module with a sub-bandgap reflector. (Adapted from [3])

Significant improvements are predicted as the device planar area is increased, since parasitic losses are reduced drastically. Moreover, the efficiency can be further enhanced through improvements in low-bandgap photovoltaics, better spectral control and higher-temperature operation [4]. Re-optimizing nanophotonic absorber–emitter surfaces, *e.g.* using 2D PhC to better match photovoltaic bandgaps, as well as using higher-temperature photonic-crystal materials such as refractory metals

could further lead to performance enhancement [5]. The efficiency improvements demonstrated in this work, as well as the promising predictions using a validated model, suggest the viability of nanophotonic STPVs for efficient and scalable solar energy conversion.

### 3. Jumping-droplet-enhanced condensation

When droplets coalesce on a superhydrophobic nanostructured surface, the resulting droplet can jump from the surface due to the release of excess surface energy. If designed properly, these superhydrophobic nanostructured surfaces can not only allow for easy droplet removal at micrometric length scales during condensation but also promise to enhance heat transfer performance. However, the rationale for the design of an ideal nanostructured surface as well as heat transfer experiments demonstrating the advantage of this jumping behavior are limited. Our work shows that silanized copper oxide surfaces (Figure 3a) created via a simple fabrication method can achieve highly efficient jumping-droplet condensation heat transfer [6].

Figure 3c compares the condensation heat transfer coefficients for conventional filmwise, flooded and dropwise condensing Cu surfaces with jumping-droplet condensation on silanized CuO superhydrophobic surfaces. It is experimentally demonstrated that a 25% higher overall heat flux and 30% higher condensation heat transfer coefficient can be achieved using jumping-droplet condensation compared to conventional dropwise condensing copper (Cu) surfaces at low super-saturations ( $S < 1.12$ ). These CuO surfaces offer ideal condensation behavior in terms of emergent droplet morphology and coalescence dynamics and a significant enhancement in heat transfer performance when compared to state-of-the-art condensing surfaces. Furthermore, the chemical-oxidation-based CuO fabrication process provides a simple and readily scalable method to create superhydrophobic condensation surfaces that can sustain droplet jumping behavior. Accordingly, these surfaces are attractive for applications such as atmospheric water harvesting and dehumidification where the heat fluxes are relatively low and droplets can be maintained in a highly mobile state.

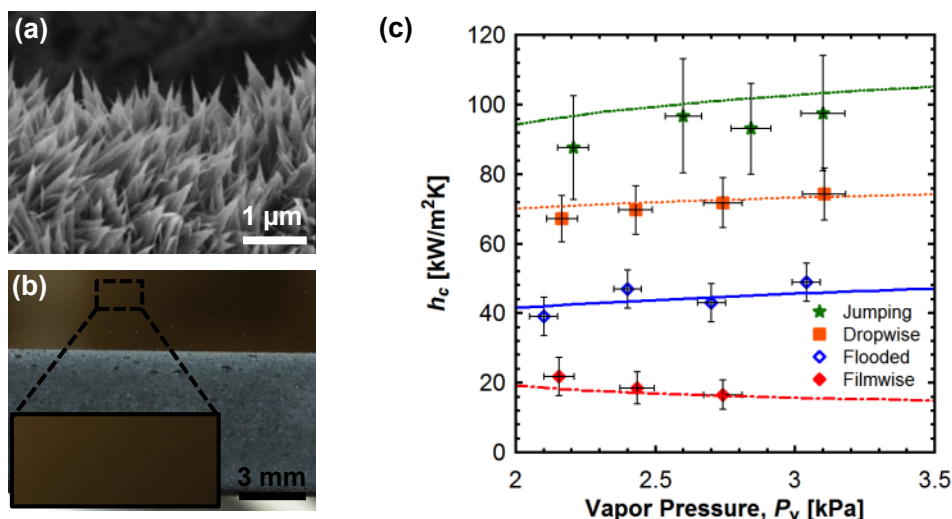


**Figure 3.** (a) Side view field emission scanning electron microscopy (FESEM) image of a CuO surface with no silane. (b) Jumping-droplet superhydrophobic condensation on a nanostructured CuO tube. (c) Experimental and theoretical steady state condensation coefficient ( $h_c$ ) as a function of saturated vapor pressure ( $P_v$ ) for tube surfaces undergoing filmwise, dropwise, flooded, and jumping condensation. (Adapted from [6])

While this droplet jumping phenomenon has been studied on a range of surfaces, past work has neglected electrostatic interactions and assumed charge neutrality of the droplets. We show that jumping droplets on a variety of superhydrophobic surfaces, including copper oxide, zinc oxide, and

silicon nanopillars, gain a net positive charge that causes them to repel each other mid-flight [7]. The charge is determined experimentally by observing droplet motion in a uniform electric field. The results show that surfaces with identical coatings, showed identical charge trends irrespective of the surface structure or surface finish which indicates that the charging of the jumping droplets occurs at the solid–liquid interface, rather than after departing from the surface. We conclude that the mechanism for the charge accumulation is associated with the formation of the electric double layer at the droplet-coating interface and subsequent charge separation during droplet jumping governed by the fast time scales of droplet coalescence.

One application of this charging phenomenon is further enhancement of condensation heat transfer by preventing droplet reversal and return to the condenser surface due to the presence of vapor flow towards the surface, which increases the drag on the jumping droplets. This effect limits the possible heat transfer enhancement because larger droplets form upon droplet return to the surface that impede heat transfer until they can be either removed by jumping again or finally shedding *via* gravity. By characterizing individual droplet trajectories during condensation on superhydrophobic nanostructured copper oxide surfaces, this vapor flow entrainment is shown to dominate droplet motion for droplets smaller than  $R \approx 30 \mu\text{m}$  at moderate heat fluxes ( $q'' > 2 \text{ W/cm}^2$ ) [8]. Subsequently, electric-field-enhanced (EFE) condensation is demonstrated, whereby an externally applied electric field prevents jumping droplet return due to the positive charge obtained by the droplets upon jumping (Figure 4). As a result, with scalable superhydrophobic CuO surfaces, a 50% higher overall condensation heat transfer coefficient is demonstrated compared to a jumping-droplet surface with no applied field for low supersaturations ( $< 1.12$ ).

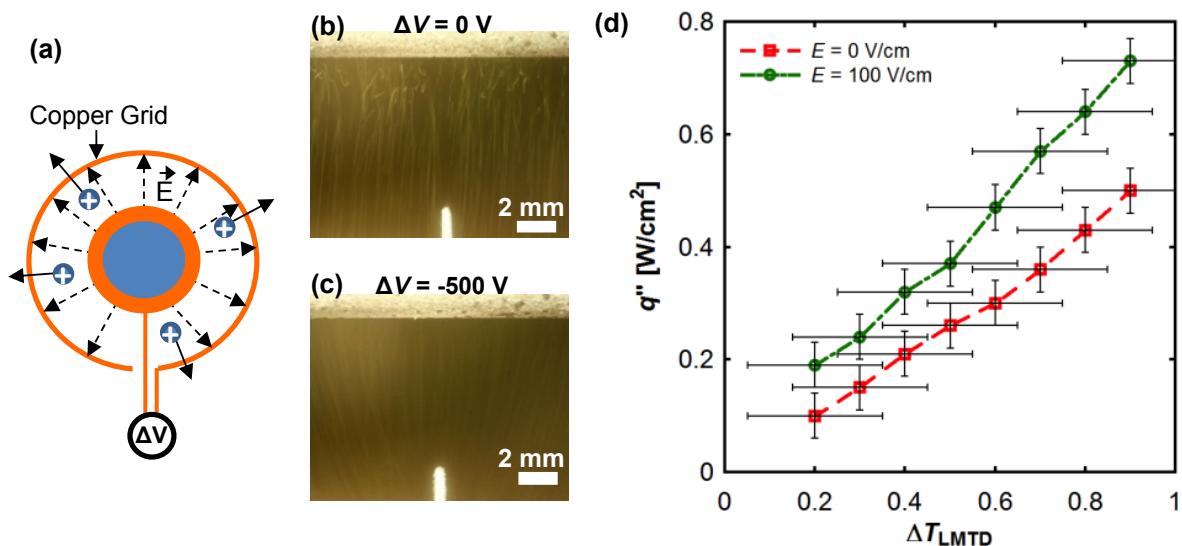


**Figure 4.** Electric-field-enhanced droplet removal. (a) Schematic of EFE condensation. The outer copper grid is biased negative relative to the condensing tube, creating an electric field and attracting jumping droplets away from the surface and preventing droplet return due to vapor flow entrainment. Long exposure time image (40 ms) of water vapor condensate on a superhydrophobic CuO tube with a copper electrode located beneath with (b) zero bias voltage having significant droplet-droplet interactions and return to the surface against gravity (pointing down) and (c) 500 V bias (electrode negative, tube ground). The image shows the concept of electric-field-enhanced (EFE) condensation with no droplet return to the surface and significant attraction of jumping droplets away from the surface ( $P_v = 2700 \pm 75 \text{ Pa}$ ,  $S \approx 1.04$ ). (d) Experimental steady-state overall surface heat flux ( $q''$ ) as a function of log mean water-to-vapor temperature difference ( $\Delta T_{\text{LMTD}}$ ) for tube surfaces undergoing jumping droplet condensation and EFE condensation. (Adapted from [8])

Another application of charged jumping droplets is use of these droplets for electrostatic energy harvesting. Here, the charged droplets jump between superhydrophobic copper oxide and hydrophilic copper surfaces to create an electrostatic potential and generate power during formation of dew under atmospheric conditions. Power densities of  $\sim 0.06$  nW/cm<sup>2</sup> were demonstrated, which, in the near term, can be improved to  $\sim 1$   $\mu$ W/cm<sup>2</sup> [9]. This work demonstrated a surface engineered platform that is low cost and scalable for atmospheric energy harvesting and electric power generation. These applications of charged jumping droplets offer new avenues for improving the performance of self-cleaning and anti-icing surfaces as well as thermal diodes, and may also provide a competitive mode of energy harvesting from temperature gradients.

#### 4. Summary

In summary, we presented an overview of the impact of using nanostructured surfaces to improve performance of solar thermophotovoltaic energy conversion and condensation systems. Our STPV system, consisting of a MWNT absorber and 1D PhC emitter with optimized nanophotonic properties, achieved experimental efficiencies of up to 3.2% in comparison to  $\leq 1\%$  reported in the literature. For condensation systems, we employed scalable superhydrophobic CuO nanostructures, among others, that can achieve significant improvements in the condensation coefficients *via* jumping-droplet condensation and electric-field-enhanced condensation modes. Furthermore, these nanostructured surfaces hold promise for several other applications including atmospheric energy harvesting, electric power generation, anti-icing and self-cleaning.

#### References

- [1] Preston D J 2014 **S.M. Thesis** Electrostatic Charging of Jumping Droplets on Superhydrophobic Nanostructured Surfaces: Fundamental Study and Applications *Department of Mechanical Engineering* Massachusetts Institute of Technology
- [2] Datas A and Algora C 2012 Development and experimental evaluation of a complete solar thermophotovoltaic system *Prog. Photovoltaics* **21** 1025-39
- [3] Lenert A, Bierman D M, Nam Y, Chan W R, Celanovic I, Soljacic M and Wang E N 2014 A nanophotonic solar thermophotovoltaic device *Nature Nanotech.* **9** 126-30
- [4] Lenert A, Nam Y, Bierman D M and Wang E N 2014 Role of spectral non-idealities in the design of solar thermophotovoltaics *Opt Express* **22** A1604-A18
- [5] Rinnerbauer V, Lenert A, Bierman D M, Yeng Y X, Chan W R, Geil R D, Senkevich J J, Joannopoulos J D, Wang E N, Soljacic M and Celanovic I 2014 Metallic Photonic Crystal Absorber-Emitter for Efficient Spectral Control in High-Temperature Solar Thermophotovoltaics *Adv. Energy Mater.* **4**
- [6] Miljkovic N, Enright R, Nam Y, Lopez K, Dou N, Sack J and Wang E N 2013 Jumping-Droplet-Enhanced Condensation on Scalable Superhydrophobic Nanostructured Surfaces *Nano Lett.* **13** 179-87
- [7] Miljkovic N, Preston D J, Enright R and Wang E N 2013 Electrostatic charging of jumping droplets *Nature Communications* **4**
- [8] Miljkovic N, Preston D J, Enright R and Wang E N 2013 Electric-Field-Enhanced Condensation on Superhydrophobic Nanostructured Surfaces *ACS Nano* **7** 11043-54
- [9] Miljkovic N, Preston D J, Enright R and Wang E N 2014 Jumping-droplet electrostatic energy harvesting *Appl. Phys. Lett.* **105**